Article:

Wang, W.-J., Lewis, S.R., Lewis, R. et al. (3 more authors) (2017) The role of slip ratio in rolling contact fatigue of rail materials under wet conditions. Wear, 376 (B). pp. 1892-1900. ISSN 0043-1648

https://doi.org/10.1016/j.wear.2016.12.049

The role of slip ratio in rolling contact fatigue of rail materials under wet conditions

W.J. Wang[a,b], S.R. Lewis[b], R. Lewis[b,*], A. Beagles[b], C.G. He[a], Q.Y. Liu[a]

a. Tribology Research Institute, Southwest Jiaotong University, Chengdu 610031, China b. Department of Mechanical Engineering, the University of Sheffield, Mappin Street, Sheffield S1 3JD, UK

Abstract: Rolling contact fatigue (RCF) of rail is a significant factor affecting the maintenance and service safety of railway track. While the driving parameters are known, clearer relationships are needed with fatigue life. The objective of this study was to explore the role of slip ratio in the development of RCF cracks and fatigue life of rail materials under a water lubricated condition. The results indicate that slip ratio has a vital and interesting influence in the wear and RCF life of rail materials. With an increase of slip ratio from 0 to 0.3%, fatigue life of rail materials has an obvious decrease. As slip ratio increases to 1%, the life increases. Then, RCF life has a drop as slip ratio changes from 1% to 5% and 10%. This may be a comprehensive effect resulting from various contact characteristics of stick area and slip area in the contact area and a competitive relationship between wear and RCF. The increase of slip ratio significantly increases the growth angle of cracks and transforms the damage mechanism of rail materials from slight surface fatigue to serious fatigue and pitting damage.

Keywords: Rail material; Slip ratio; Rolling Contact Fatigue; Fatigue life; Wear

1. Introduction

As the wheel/rail is an opening system, many factors affect the contact behaviour in the wheel/rail interface. The wear and RCF of rail as major damage types often occur in the

*Corresponding author. Tel: +44-114-2227838.

E-mail address: Roger.Lewis@sheffield.ac.uk (R. Lewis).

wheel/rail contact and play a vital role in influencing the safety and maintenance of railway track. It is noted that many oblique fatigue cracks appear on the railway wheel and rail surfaces, which can result in complete failure of rail and potential derailment. As reviewed in previous literature, lots of factors such as wheel and rail materials, lubricants, contact parameters (contact pressure, slip ratio, axle load, curve radius, etc.), operating environment (water, snow, low temperature), have a significant influence on wear and RCF of wheel and rail materials [1-4]. Therefore, the formation mechanism and controlling measures of RCF and related defects of wheel/rail are an ongoing concern for many researchers.

It is well known that the microstructure of materials determines the wear and RCF performances of wheel/rail [5-7]. Meanwhile, the initiation and propagation of RCF cracks is always affected by the microstructure of materials [8-10]. The deformed microstructure influences the RCF crack initiation in rail and it is found that surface cracks primarily initiate along the more highly strained, proeutectoid ferrite phase boundaries [11]. In recent years, the development of steel making technology has substantially reduced RCF defects associated with non-metallic oxide inclusions and hydrogen shatter cracking [12]. The decrease of lamellar spacing of pearlitic rail contributes to improving the wear and RCF resistance. Some premium rail steels exhibit pro-eutectoid cementite at the prior austenite grain boundaries, for example the new rail material with better RCF resistance, developed by Ordonez Olivares et al. [13]. However, it is noted that wear mass losses from a disc-on-disc testing are similar for bainitic and pearlitic microstructures regardless of their initial hardness [14]. Decarburization often appears on the rail surface due to fact that the oxidization of carbon is faster than that of iron in the hot rolling process [15]. Evidence is provided to show that the effect of decarburization on the rail surface on RCF is to increase the crack growth rate of samples with increasing depth [15-16]. Furthermore, the crack propagating mechanisms are different between the non-decarburized and decarburized rail materials [16].

Moreover, various lubricants (oil, grease, friction modifier, etc.) are frequently used to decrease the wear of the wheels and rails and significantly influence the initiation and growth of rolling contact fatigue cracks. The performance of different grease types as curve lubricants was assessed and there is an inverse relationship between retentivity and disc wear rate [17]. Hardwick has produced a new $T\gamma$ wear curve and creep curve for 260 grade rail and R8T wheel materials using a twin disc testing technique under the dry, water and grease lubrication conditions [18]. Water is commonly present in the wheel/rail interface and greatly reduces the wear of wheel/rail and transforms the damage mechanism of the wheel and rail materials [19]. The application of friction modifiers greatly reduces the wear of the rail head [20]. Hardwick found that the application of lubrication accelerates the propagation of pre-existing cracks and the increase of RCF damage is closely related to the viscosity of the lubricants [1]. The growth speed of RCF cracks is the fastest when water is applied. A numerical technique has also been used to estimate the effect of lubricant on the stress intensity factors (SIF) of rolling contact fatigue cracks in the rolling-sliding contact [21].

In the wheel/rail contact, both rolling and sliding always occurs in the contact area. On a straight track, the wheel tread is in contact with the rail head, but in curves the wheel flange may be in contact with the gauge corner of the rail. Therefore, the stick area (no relative sliding) and slip area can be found in the wheel/rail contact zone. With the slip ratio increasing, the wear mechanism of wheel and rail materials transforms from slight oxidation wear to severe fatigue wear and spalling damage [22]. On the other hand, fatigue strength obtained by RCF tests decreases with the increase in the slip ratio [23]. The slip ratio also affects the minimum crack size for growth in a rolling-sliding contact [24].

It is a fact that slip ratio varies in the wheel/rail contact, which could bring an important influence on RCF crack characteristics of rail materials. Clayton and Hill [25] have found that there is an interesting result for the relationship between the creepage and RCF life. However, the explanation of why this variation occurs needs further clarification. In view of this, the effect of slip ratio on rolling contact fatigue of rail materials was studied under wet conditions using a twin disc machine. Particularly, the propagation characteristics of RCF cracks were explored using various micro-examinations.

2. Experimental details

RCF testing was performed on the Sheffield University Rolling Sliding (SUROS) twin-disc tester. Details of its capabilities and usage have been described in the literature [26]. It is based on a Colchester Mascot lathe with an independently driven AC motor at the tailstock end, shown in Fig.1. A torque transducer mounted on one of the shafts continually monitors the torque. A load sensor (accuracy: ±2%) mounted beneath the hydraulic jack is used to measure the required normal load. Slip ratios are achieved by means of alteration of the rotational speed of the AC motor. The wheel disc (lower roller) acts as a driving disc and the rail disc (upper roller) acts as the brake for simulating the traction state.

The wheel and rail rollers were cut from R8T wheel rim and 260 grade rail head parallel, and as close as possible to the outer surface. All rollers were machined to a diameter of 47 mm with a contact width of 10 mm. A rotational speed of 400 r/min and a maximum contact pressure of 1500 MPa from a normal load of about 7.14 kN were used. In the testing process, water was added to the surface of rail disc using a channel at a rate of about 2 drops per second. The slip ratios used were 0, 0.3%, 1%, 5% and 10%.

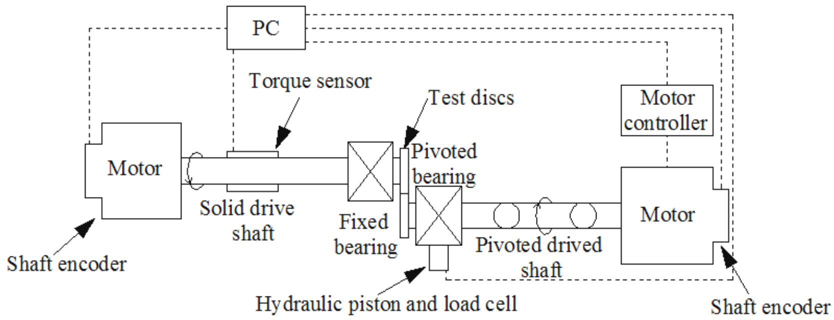

Fig.1. SUROS twin-disc tester.

All tests were run under dry conditions first for 500 cycles at 1% slip ratio in order to initiate RCF damage on the rail disc surfaces. This was followed by wet testing at different slip ratios. This is a standard approach to RCF testing on the SUROS machine [25]. An eddy current crack detection system was used to monitor the growth of cracks with increasing cycles [27]. A differential eddy current probe (accuracy: 10 μm) (Fig.2a) was connected to the detector about 0.3 mm from the surface of the rail roller. RCF failure definition was set using a calibration rail disc with wire eroded reference cracks in the disc surface [27-28]. When a calibration rail disc was rotated in the calibration experiment, the signal of the eddy current probe as a reference signal was displayed on the detector screen (Fig.2b). When the signal of cracks in the testing discs reached the reference signal (Fig.2b), the test was stopped and RCF life of rail materials was obtained.

Testing was performed under an ambient temperature of 20~22 ℃ and humidity of 30~40%. The wear rates (mass loss (μg) per rolling cycle) of rail rollers were measured by an electronic balance (accuracy: 0.1 μg) and the first weighing was achieved before the dry testing. The hardness was measured using a Vickers hardness instrument (MVK-H21, Japan). The damaged surfaces and longitudinal sections cut along the rolling direction were examined using scanning electronic microscopy (SEM) (JSM-7001F, Japan) and optical microscopy (OM) (OLYMPUS BX60M, Japan).

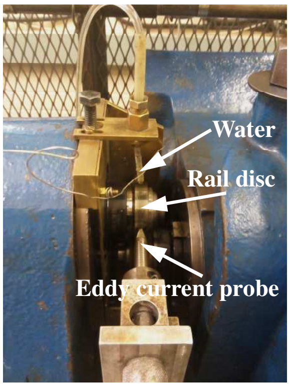

(a)

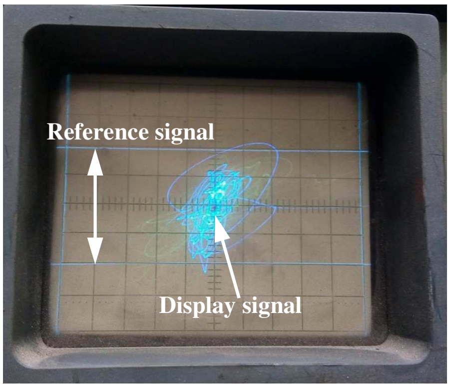

(b)

Fig.2. Eddy current crack detection system, (a) eddy current probe; (b) detector signal.

3. Results

3.1 Traction coefficient and fatigue life

Traction coefficients of wheel/rail discs under wet conditions are shown in Fig.3 and it is found that, after a settling-in period, the traction coefficients remain fairly constant with an increase in the number of cycles (Fig.3a). With an increase of slip ratio from 0 to 1 %, the steady-state traction coefficient rapidly increases due to the increase of micro-slip in the contact zone, shown in Fig.3b (the value is average traction coefficient during the wet period for each test). Furthermore, average traction coefficient is stable before there is a small fall as slip ratio changes from 1% to 5% and 10% under the wet condition.

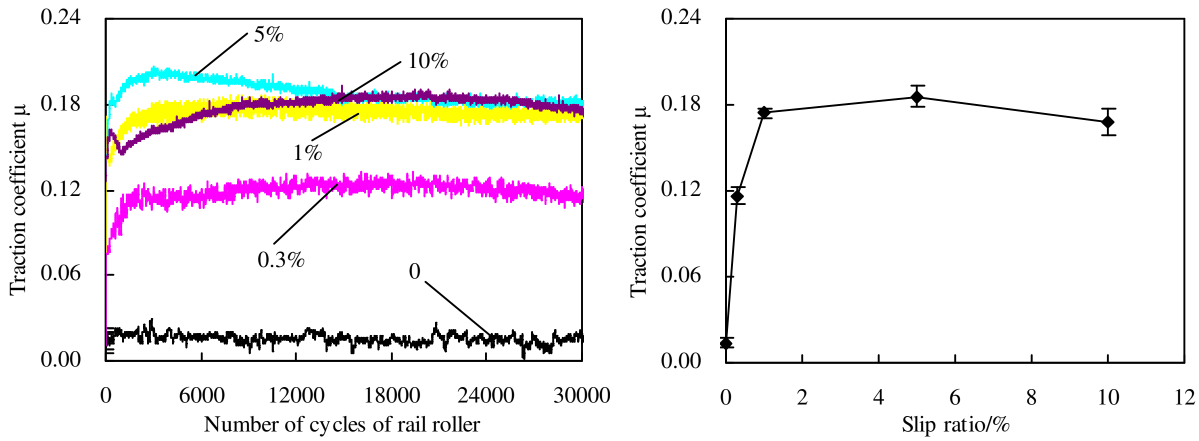

(a) (b)

Fig.3. Traction coefficient of wheel/rail discs under wet condition, (a) dynamic traction coefficient; (b) average traction coefficient.

An interesting result about the fatigue life of rail discs is given in Fig.4. As slip ratio slightly increases to from 0 to 0.3%, the fatigue life falls. Then, RCF life of the rail discs increases when slip ratio is increased to 1%. However, there is a further drop as slip ratio changes from 1% to 5%. As slip ratio increases further to 10%, the RCF life does not seem to change.

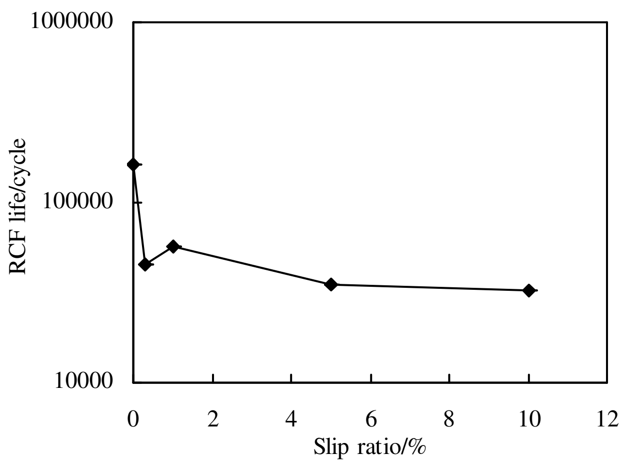

Fig.4. RCF life of rail discs vs. slip ratio.

3.2 Wear and surface damage

It is visible from Fig.5 that the wear rate of rail discs rapidly increases with the slip ratio increasing from 0 to 0.3%. As the slip ratio further increases to 1%, the wear rate of the rail disc slightly falls. When the slip ratio changes from 5% to 10%, the wear rate also has an obvious drop. It is noted that the wear rate is closely related to the change of the traction force in the wheel/rail interface under wet conditions as slip is created. It should be noted that the wear transition from mild wear to severe wear may be caused by the increase of slip ratio in the wheel/rail interface under dry conditions [29]. However, the wear rate of the rail disc in this study peaks under the 0.3% slip ratio condition. The expected reason may be high crack growth rate (low RCF life in Fig.4) resulting in more material removal from the rail disc at 0.3% slip ratio under wet conditions. So, the wear mechanism in this case is different from the dry condition under the same slip ratio condition.

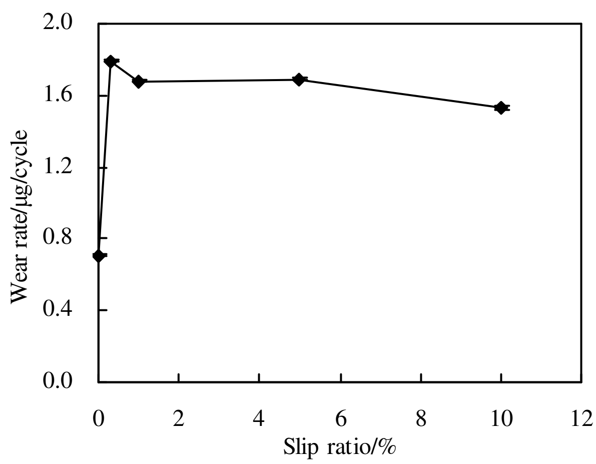

Fig.5. Wear rate of rail discs vs. slip ratio.

SEM microscopic observation of surface damage on the rail discs in Fig.6 shows that the surface damage is very slight and that there is slight fatigue when the slip ratio is zero (Fig.6a). With the slip ratio increases to 0.3% and 1%, some thin metal tongues are found on the surface of the rail discs (Fig.6b and c) and the fatigue effects are more obvious. When the slip ratio further increases to 5% and 10%, the surface damage becomes more serious and the fatigue is significant on the surface of rail discs. Furthermore, slight pitting appears on the rail disc's surface when the largest slip ratio (10%) is applied. The experimental results show that the surface damage of rail discs with dry pre-testing of 500 cycles under wet conditions is remarkably affected by the slip ratio in the wheel/rail contact. With the slip ratio increasing from 0 to 10%, the damage of rail discs increases and the damage mechanism transforms from slight surface fatigue to serious fatigue and slight pitting damage. However, the wear rate of the rail discs has no obvious change as the slip ratio increases from 1% to 5%. The reason may be explained that after the full slip condition has been reached, increasing slip ratio further then has no effect on the wear [29].

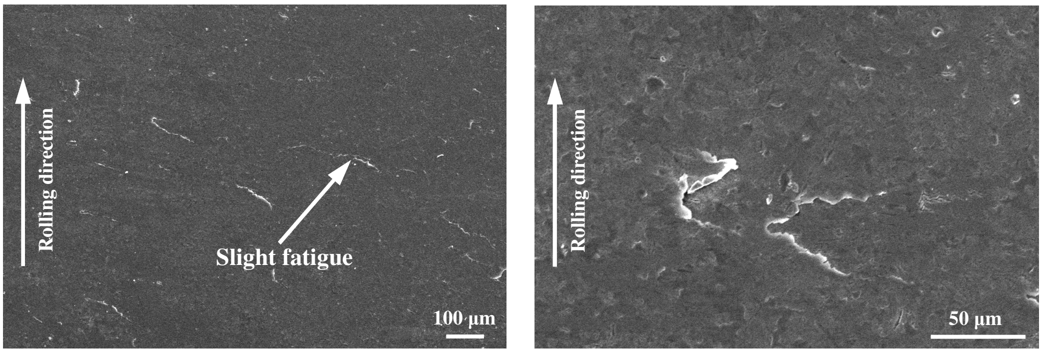

(a)

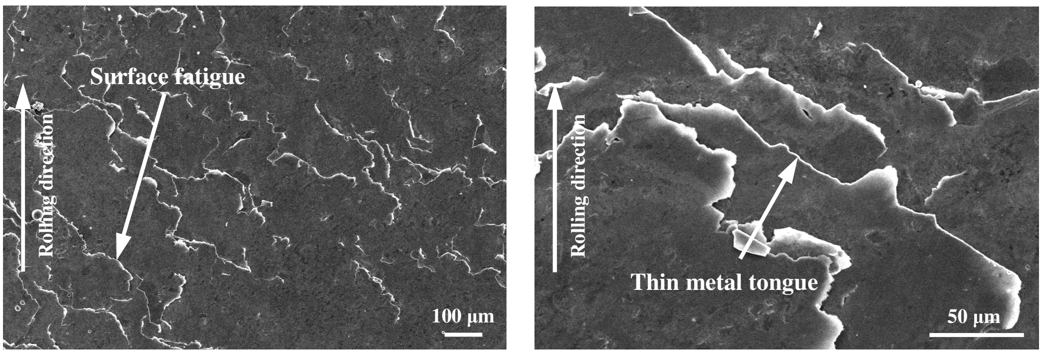

(b)

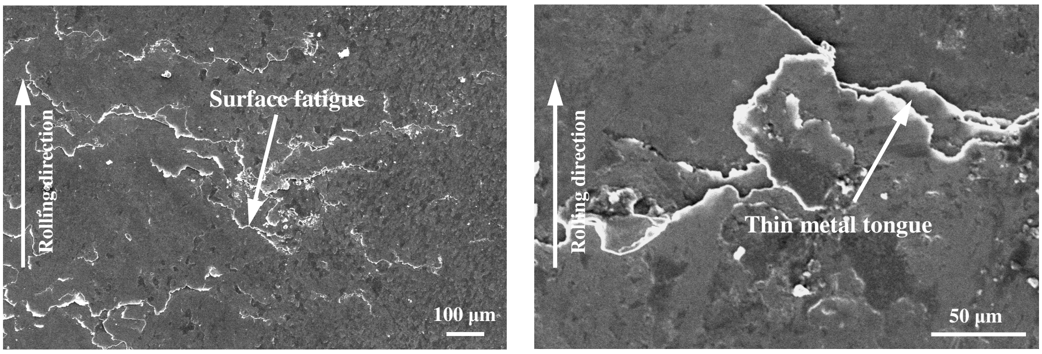

(c)

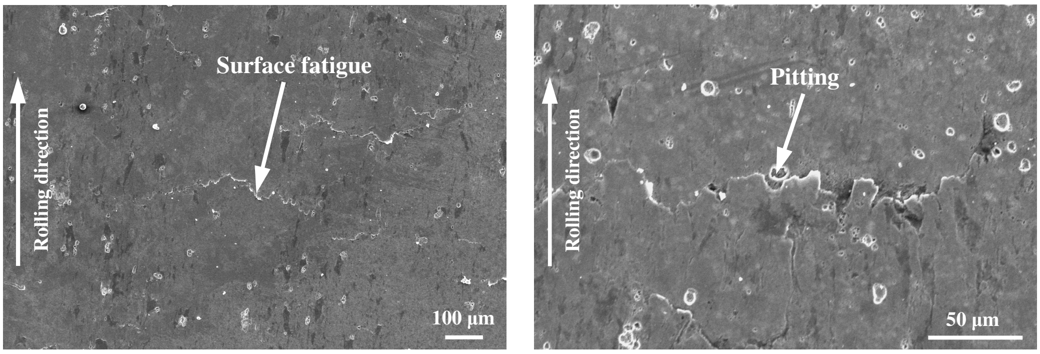

(d)

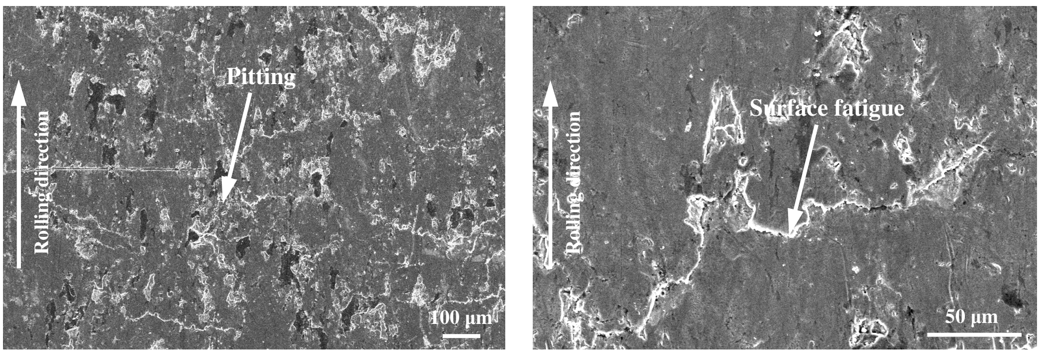

(e)

Fig.6. SEM micrographs of surface damage of rail discs, (a) 0; (b) 0.3%; (c) 1%; (d) 5%; (e) 10%.

It is well known that the hardness variation of the sections reflects the sub-surface shear deformation of rail materials, shown in Fig.7. The hardness rapidly increases and reaches a maximum as the depth below the surface increases, with the depth of the peak hardness decreasing with increasing slip. Then, the hardness gradually decreases and nears the bulk value of the rail materials with further increase in the distance from surface. Under the wet condition, the traction coefficient of wheel/rail discs is less than 0.2 (Fig.3). So, the maximum hardening shear stress is located below the surface of the rail discs (Fig.8). Furthermore, there is no visible sub-surface deformation layer due to very small traction force in the wheel/rail interface when the slip ratio is zero (Fig.8a). It is obvious in Fig.8c that the depth of plastic deformation layer rapidly increases with the rise in slip ratio from 0 to 0.3% and then a slight increase with further increase to 10%. There is a similar change in the surface damage of the rail discs with the increase in slip ratio.

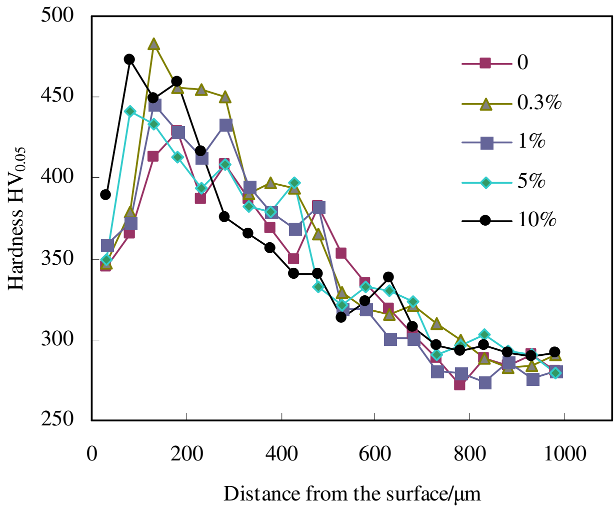

Fig.7. Hardness of rail discs vs. the distance from surface.

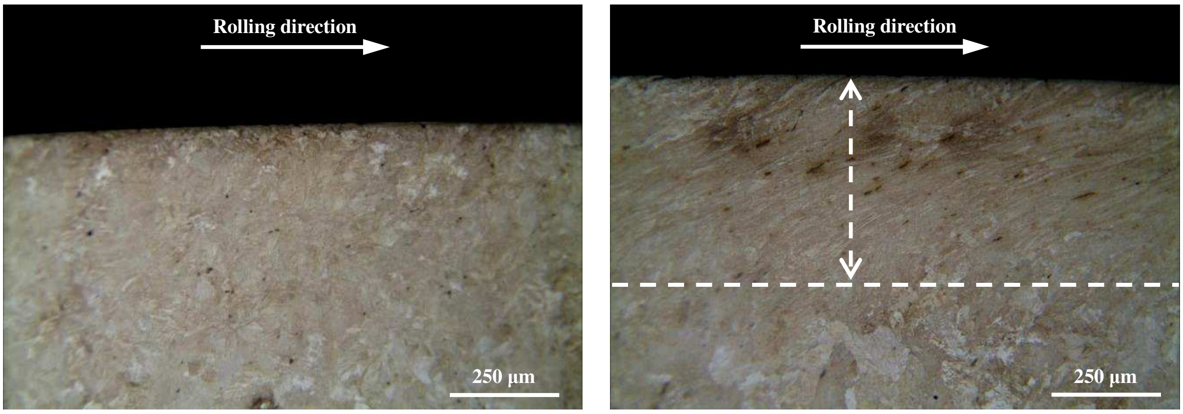

(a) (b)

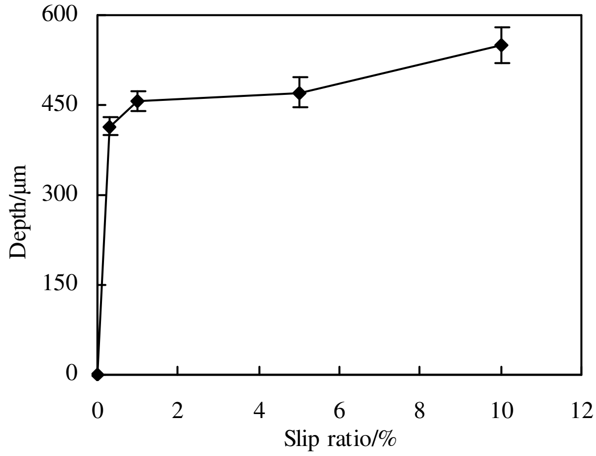

(c)

Fig.8. OM micrographs of plastic deformation of rail discs, (a) 0; (b) 5%; (c) depth vs. slip ratio.

3.3 RCF cracks behaviour

OM microscopic observation in Fig.9a shows that there is no visible fatigue crack when the slip ratio is zero. It should be noted that the traction force in the wheel/rail interface has a vital role in the formation of RCF crack [30]. As the traction force is very small, it is very difficult to initiate cracks under wet conditions. It is worth noting that pure rolling is not actually achieved in the testing process. Actual RCF life of the rail disc should be far more than experimental data in Fig.4 when the slip ratio is zero. With the slip ratio increasing, many cracks can be found sub-surface of the rail discs (Fig.9b).

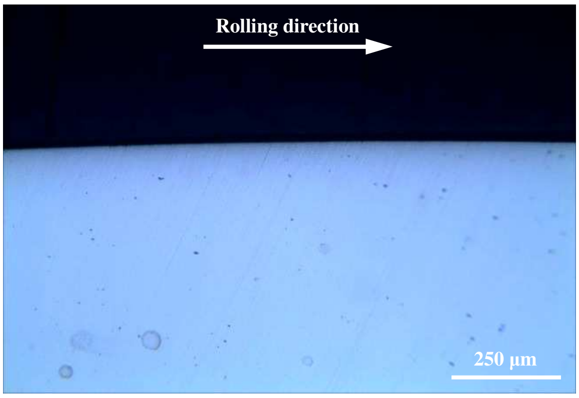

(a)

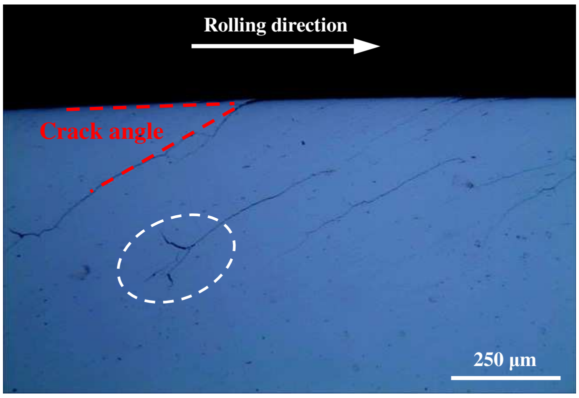

(b)

Fig.9. Typical fatigue cracks of rail discs, (a) 0; (b) 1%.

Figs.10~13 give higher magnification SEM micrographs of fatigue cracks of the rail discs. It is obvious that many cracks are parallelly distributed along the deformation line of the rail discs and grow at a certain angle. It should be noted that the length of RCF cracks varies, however, it is found that the maximum length of cracks under different slip ratio conditions is almost the same. In the crack growth process, there are many branch cracks (Figs.10 and 11). When 0.3% slip ratio is applied, multi-layer cracks are found. With the slip ratio increasing (5% and 10%), annular branch cracks appear due to the connection of branch cracks (Figs.12 and 13). It is worth noting that the formation of branch and annular cracks is affected by the deformation of the rail discs. When the slip ratio increases from 0.3% to 1%, the depth of the deformation layer (Fig.8c) and branch cracks (Figs.10 and 11) both increase. Furthermore, when the slip ratio increases from 5% to 10%, the deformation of the rail discs becomes more and more serious, which means that more annular cracks appear (Figs.12 and 13). It is clear in Fig.14 that the growth angle of RCF cracks (crack angle is the included angle between parallel surface direction and crack growth direction, shown in Fig.9b) is significantly different under different slip ratio conditions. The maximum and average of crack angle of the rail discs obviously increases with the slip ratio increasing.

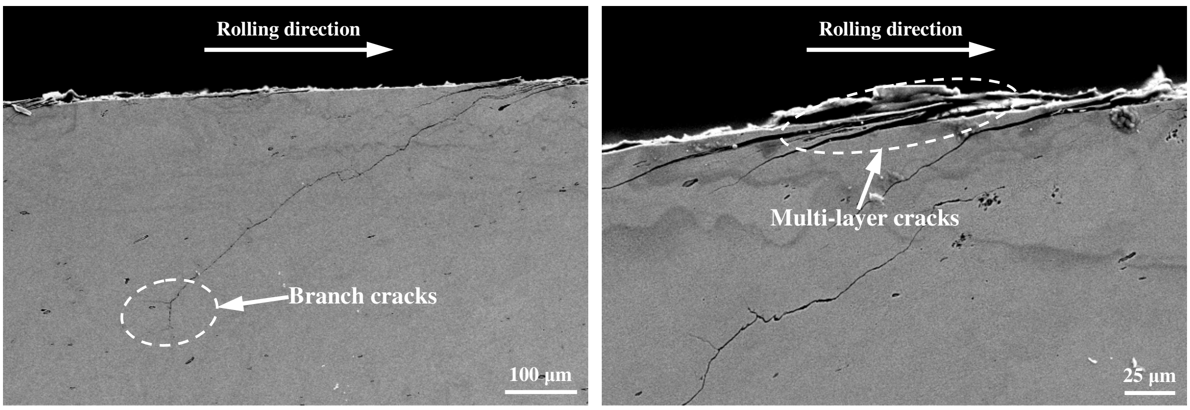

Fig.10. SEM micrographs of fatigue cracks of rail discs at slip ratio of 0.3%.

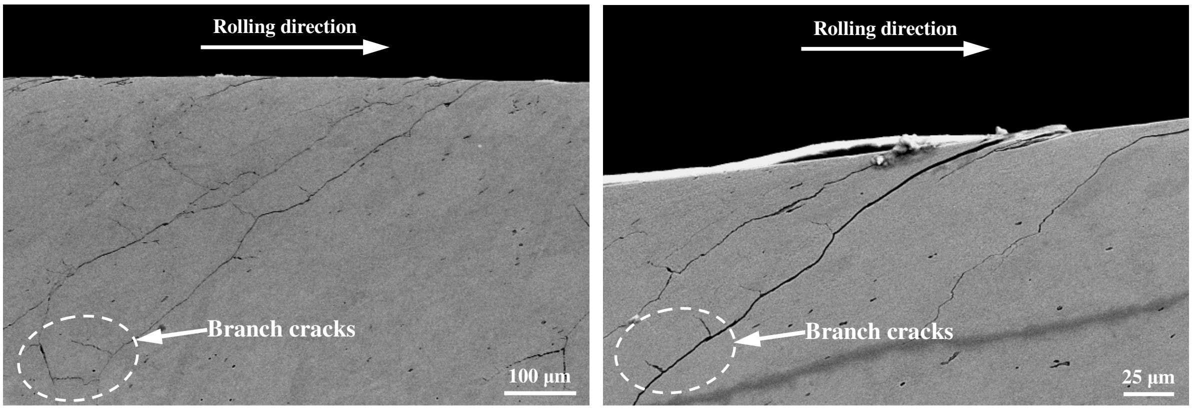

Fig.11. SEM micrographs of fatigue cracks of rail discs at slip ratio of 1%.

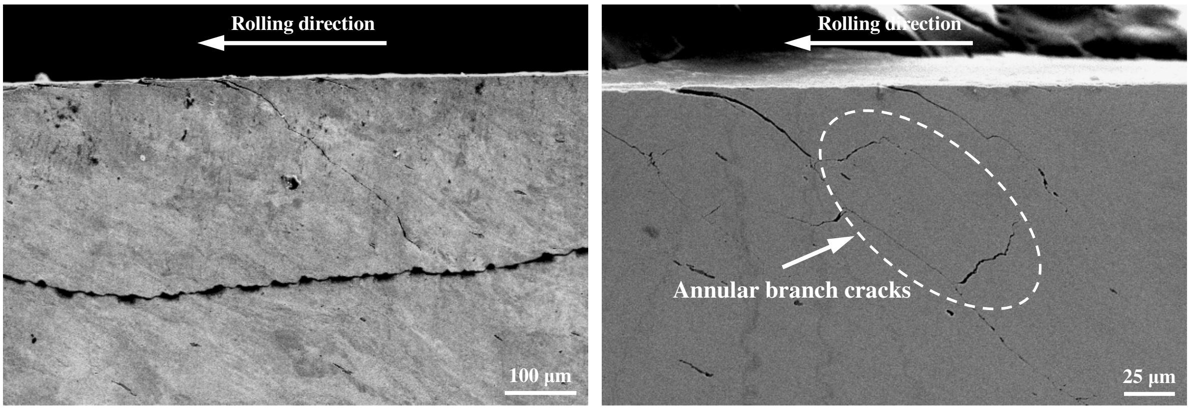

Fig.12. SEM micrographs of fatigue cracks of rail discs at slip ratio of 5%.

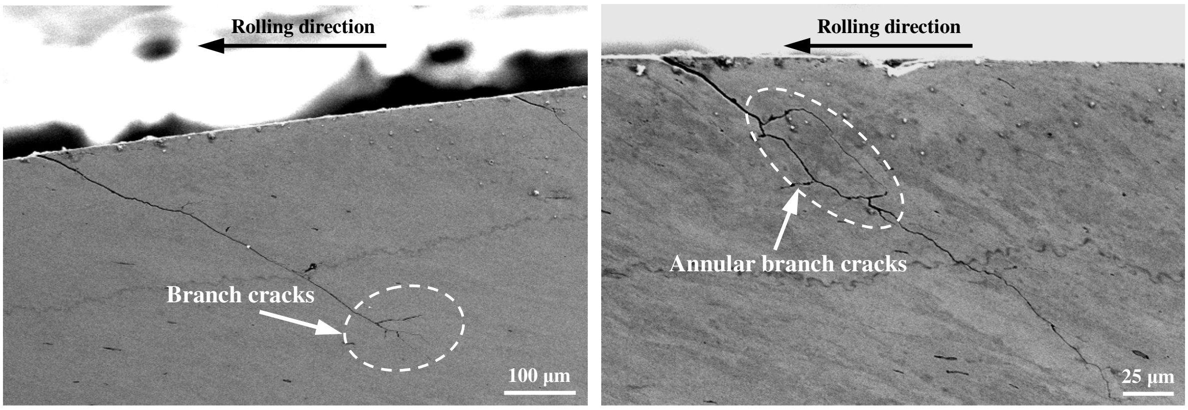

Fig.13. SEM micrographs of fatigue cracks of rail discs at slip ratio of 10%.

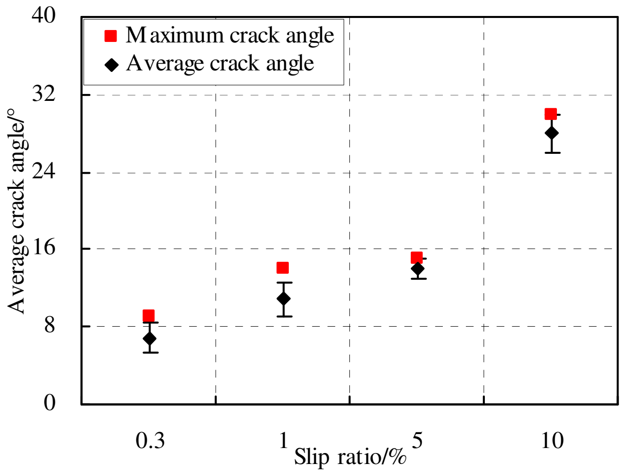

Fig.14. Crack angle of rail discs vs. slip ratio.

4. Discussion

In this study, pre-testing with 500 cycles at 1% slip ratio under dry condition was carried out for initiating initial slight RCF damage on the rail disc surfaces. Previous test results indicated that initial dry cycling significantly affects the RCF life under wet conditions [31]. Furthermore, water accelerates the growth of rolling contact fatigue cracks of the wheel and rail discs with pre-existing initial damage [32]. In the rolling-sliding process, water could easily enter the initial surface cracks of rail discs and then, as an incompressible fluid, will be sealed and trapped in the crack mouth. This causes a rapid growth of cracks due to a hydraulic crack growth mechanism, shown in Fig.15a. With the cycling number increasing, the length of cracks will constantly increase by means of hydraulic crack growth in Mode I. In this crack growth mechanism, the viscosity of lubricants plays a vital role in the growth rate of cracks. Hardwick [1] has explored the influence of different friction modifiers on the crack propagation and found that a lower viscosity product causes accelerated crack growth of rail materials.

It is noted that the crack growth needs a driving force in the cyclic normal load process. The stress intensity factor of crack growth is affected by many factors in the contact surface and crack face [33]. The traction coefficient is the most dominant parameter in the determination of minimum crack size for growth [24] and this means that there is a different driving force of crack growth under different traction coefficient conditions. When the slip ratio is zero, the traction force in pure rolling contact is very small, so it is difficult to provide a sufficient driving force for crack growth. So, RCF life is very long. When slip ratio increases to 0.3%, the increase of traction force results in an obvious decrease of RCF life (Fig.4). Increasing slip ratio would change the distribution of stick and slip area (Fig.15b) and the stick area decreases and the slip area increases with the slip ratio increasing. In this process, the increase of slip area in the contact zone may cause the decrease of driving force from the hydraulic crack growth owing to the decrease of crack fluid. So, RCF life of the rail disc would increase when the slip ratio increases from 0.3% to 1%. Once the slip ratio exceeds 1%, the stick area will always disappear and full slip area exists in the wheel/rail contact zone. So, increasing relative sliding velocity of wheel/rail discs leads to an increase in the driving force of crack growth, which makes RCF life of the rail discs at 5% and 10% slip ratios to fall compared with 1% slip ratio condition. It is worth noting that similar experimental results were also obtained by Clayton and Hill [25] by means of a water-lubricated RCF testing without pre-existing RCF cracks. However, the rollers in this case were lubricated by the water all the while during the testing and the experimental method is not same compared with this study. Furthermore, no in-depth explanation in Clayton and Hill's study was given for this effect in their work.

On the other hand, the relation between damage factor and $T\gamma$ value also affect the RCF characteristics of the rail discs, shown in Fig.15c [34]. When $T\gamma$ value is small, low wear rate occurs and the RCF damage dominates and so the RCF life is short (slip ratio is less than 0.3% in this study). After the $T\gamma$ value reaches a critical point, the wear increases and dominates. So, the RCF life will increase (e.g. 1% slip ratio). Furthermore, it is worth noting that the higher temperatures associated with 5% and 10% slip during testing in the contact zone may reduce the RCF life of rail materials. In summary, the variation of RCF life versus slip ratio in this study may be a complicated and comprehensive effect resulting from various contact characteristics of stick area and slip area in the wheel/rail contact zone (resulting in different hydraulic crack growth effect, contact temperature) and a competitive relation between RCF and wear damage and $T\gamma$ value.

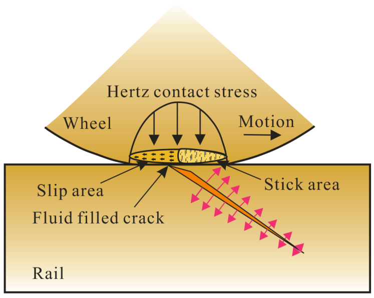

(a)

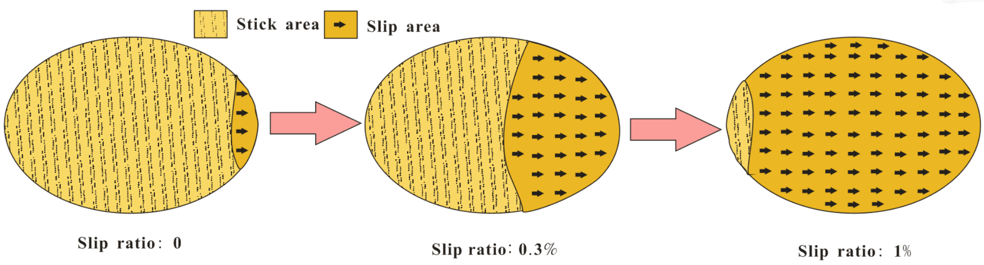

(b)

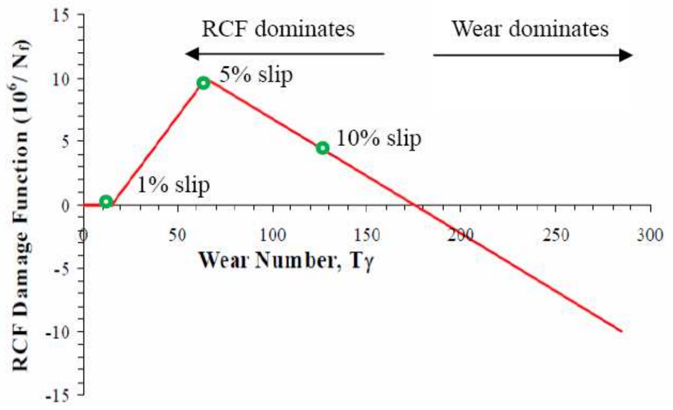

(c)

Fig.15. (a) Schematic representation of crack growth under the wet condition; (b) distribution of contact zone vs. slip ratio; (c) the relation between damage and $T\gamma$ value [34].

Furthermore, the growth of branch cracks based on Mode I was explored by Wong [35]. The stress intensity factor of crack tip would significantly affect the growth path and direction of crack. In this case, the increase of slip ratio obviously increases the growth angle of cracks. It is worth pointing out that many factors influence the crack propagation characteristics under the fluid lubrication condition. In view of understanding the dynamic crack growth behaviour, further work on the crack growth driving force, stress intensity factor and propagation path should be calculated and evaluated using crack modelling under different slip ratio conditions.

5. Conclusions

This experimental study explored the role of slip ratio in RCF cracks and fatigue life of rail materials under a water lubricated condition. The following conclusions were obtained:

1. Slip ratio has a significant and interesting influence in the wear and RCF life of rail materials owing to various contact characteristics of stick area and slip area in the wheel/rail

contact and a competitive relation between damage and $T\gamma$ value. With the slip ratio increasing from 0 to 10%, the damage mechanism of rail discs transforms from slight surface fatigue to serious fatigue and slight pitting damage.

2. With an increase in slip ratio from 0 to 0.3%, the RCF life of rail materials has an obvious decrease. As slip ratio increases to 1%, RCF life increases. Then, RCF life has a drop as slip ratio changes from 1% to 5% and 10%.

3. Under a dry 500 cycles pre-testing condition, water accelerates the crack growth due to hydraulic crack growth mechanism, which results in the appearance of branch cracks and annular branch cracks. The increase of slip ratio significantly increases the growth angle of RCF cracks.

Acknowledgments

The work is supported by the National Natural Science Foundation of China (No.51475393). The first author would thank the State Scholarship Fund of the China Scholarship Council (CSC) (No.201407005021), to pursue study in the University of Sheffield as an Academic Visitor.

References

[1] C. Hardwick, R. Lewis, The effects of alternative top of rail friction materials on pre-existing rolling contact fatigue cracks, In: Proceedings of the Second International Conference on Railway Technology: Research, Development and Maintenance, J. Pombo, (Editor), Civil-Comp Press, Stirlingshire, Scotland, (2014) 1-17.

[2] M. Steenbergen, Rolling contact fatigue in relation to rail grinding, Wear 356-357 (2016) 110-121.

[3] A. Ekberg, B. Åkesson, E. Kabo, Wheel/rail rolling contact fatigue-probe, predict, prevent, Wear 314 (2014) 2-12.

[4] H.H. Ding, C.G. He, L. Ma, J. Guo, Q.Y. Liu, W.J. Wang, Wear mapping and transitions in wheel and rail materials under different contact pressure and sliding velocity conditions, Wear 352-353 (2016) 1-8.

[5] J.W. Seo, H.K. Jun, S.J. Kwon, D.H. Lee, Rolling contact fatigue and wear of two different rail steels under rolling-sliding contact, Int. J. Fatigue 83 (2016) 184-194.

[6] D. Benoît, B. Salima, R. Marion, Multiscale characterization of head check initiation on rails under rolling contact fatigue: Mechanical and microstructure analysis, Wear 366-367 (2016) 383-391.

[7] R. Stock, R. Pippan, RCF and wear in theory and practice-the influence of rail grade on wear and RCF, Wear 271 (2011) 125-133.

[8] S. Maya-Johnson, A.J. Ramirez, A. Toro, Fatigue crack growth rate of two pearlitic rail steels, Engineering Fracture Mechanics 138 (2015) 63-72.

[9] F.J. Franklin, A. Gahlot, D.I. Fletcher, J.E. Garnham, C. Davis, Three-dimensional modelling of rail steel microstructure and crack growth, Wear 271 (2011) 357-363.

[10] H. Yokoyama, S. Mitao, S. Yamamoto, M. Fujika, Effect of the angle of attack on flaking behavior in pearlitic and bainitic steel rails, Wear 253 (2002) 60-66.

[11] J.E. Garnham, C.L. Davis, The role of deformed rail microstructure on rolling contact fatigue initiation, Wear 265 (2008) 1363-1372.

[12] D.F. Cannon, H. Pradier, Rail rolling contact fatigue research by the European Rail Research Institute, Wear 191 (1996) 1-13.

[13] R. Ordonez Olivares, C.I. Garcia, A. DeArdo, S. Kalay, F.C. Robles Hernandez, Advanced metallurgical alloy design and thermomechanical processing for rails steels for North American heavy haul use, Wear 271 (2011) 364-373.

[14] D. Zapata, J. Jaramillo, A. Toro, Rolling contact and adhesive wear of bainitic and pearlitic steels in low load regime, Wear 271 (2011) 393-399.

[15] R.I. Carroll, J.H. Beynon, Decarburisation and rolling contact fatigue of a rail steel, Wear 260 (2006) 523-537.

[16] X.J. Zhao, J. Guo, H.Y. Wang, Z.F. Wen, Q.Y. Liu, G.T. Zhao, W.J. Wang, Effects of decarburization on the wear resistance and damage mechanisms of rail steels subject to contact fatigue, Wear 364-365 (2016) 130-143.

[17] S.R. Lewis, R. Lewis, G. Evans, L.E. Buckley-Johnstone, Assessment of railway curve lubricant performance using a twin-disc tester, Wear 314 (2014) 205-212.

[18] C. Hardwick, R. Lewis, D.T. Eadie, Wheel and rail wear-understanding the effects of water and grease, Wear 314(2014) 198-204.

[19] W.J. Wang, R. Lewis, B. Yang, L.C. Guo, Q.Y. Liu, M.H. Zhu, Wear and damage transitions of wheel and rail materials under various contact conditions, Wear 362-363 (2016) 146-152.

[20] D.T. Eadie, D. Elvidge, K. Oldknow, R. Stock, P. Pointner, J. Kalousek, P. Klauser, The effects of top of rail friction modifier on wear and rolling contact fatigue: Full-scale rail-wheel test rig evaluation, analysis and modelling, Wear 265 (2008) 1222-1230.

[21] M. Dallago, M. Benedetti, S. Ancellotti, V. Fontanari, The role of lubricating fluid pressurization and entrapment on the path of inclined edge cracks originated under rolling-sliding contact fatigue: Numerical analyses vs. experimental evidences, Int. J. Fatigue 92 (2016) 517-530.

[22] L. Ma, C.G. He, X.J. Zhao, J. Guo, Y. Zhu, W.J. Wang, Q.Y. Liu, X.S. Jin, Study on wear and rolling contact fatigue behaviors of wheel/rail materials under different slip ratio conditions, Wear 366-367 (2016) 13-26.

[23] T. Makino,T. Kato, K. Hirakawa, The effect of slip ratio on the rolling contact fatigue property of railway wheel steel, Int. J. Fatigue 36 (2012) 68-79.

[24] H.K. Jun, D.H. Lee, D.S. Kim, Calculation of minimum crack size for growth under rolling contact between wheel and rail, Wear 344-345 (2015) 46-57.

[25] P. Clayton, D.N. Hill, Rolling contact fatigue of a rail steel, Wear 117 (1987) 319-334.

[26] D.I. Fletcher, J.H. Beynon, Development of a machine for closely controlled rolling contact fatigue and wear testing, J. Test. Eval. 28 (2000) 267-275.

[27] S.R. Lewis, R. Lewis, D.I. Fletcher, Assessment of laser cladding as an option for repairing/enhancing rails, Wear 330-331 (2015) 581-591.

[28] J.E. Garnham, J.H. Beynon, The early detection of rolling-sliding fatigue cracks, Wear 144 (1991) 103-116.

[29] R. Lewis, R.S. Dwyer-Joyce, Wear mechanisms and transitions in railway wheel steels, Proc. Inst. Mech. Eng. Part J: J. Eng. Tribol. 218(6) (2004) 467-478.

[30] C.G. He, Y.B. Huang, L. Ma, J. Guo, W.J. Wang, Q.Y. Liu, M.H. Zhu, Experimental investigation on the effect of tangential force on wear and rolling contact fatigue

behaviors of wheel material, Tribol. Int. 92 (2015) 307-316.

[31] W.R. Tyfour, J.H. Beynon, A. Kapoor, Deterioration of rolling contact fatigue life of pearlitic rail steel due to dry-wet rolling-sliding line contact, Wear 197(1-2) (1996) 255-265.

[32] J.H. Beynon, J.E. Garnham, K.J. Sawley, Rolling contact fatigue of three pearlitic rail steels, Wear 192 (1996) 94-111.

[33] A.F. Bower, The influence of crack face friction and trapped fluid on rolling contact fatigue cracks, ASME Journal of Tribology 110 (1988) 704-711.

[34] M.C. Burstow, Whole life rail model application and development for RSSB-development of an RCF damage parameter, AEA Technology Rail report AEATR-ES-2003-832 Issue 1, www.rssb.co.uk, (2003).

[35] S.L. Wong, P.E. Bold, M.W. Brown, R.J. Allen, A branch criterion for shallow angled rolling contact fatigue cracks in rails, Wear 191 (1-2) (1996) 45-53.